HHS Public Access

Author manuscript

Pediatr Blood Cancer. Author manuscript; available in PMC 2016 January 01.

Published in final edited form as:

Pediatr Blood Cancer. 2015 January ; 62(1): 91–98. doi:10.1002/pbc.25201.

Initial Testing (Stage 1) of the PARP Inhibitor BMN 673 by the Pediatric Preclinical Testing Program: PALB2 Mutation Predicts Exceptional in Vivo Response to BMN 673

Malcolm A. Smith, MD, PhD[1], **Oliver A. Hampton, PhD**[2,3], **C. Patrick Reynolds, MD, PhD**[4], **Min H. Kang, PharmD**[4], **John M. Maris, MD**[5], **Richard Gorlick, MD**[6], **E. Anders Kolb, MD**[7], **Richard Lock, PhD**[8], **Hernan Carol, PhD**[8], **Stephen T. Keir, PhD**[9], **Jianrong Wu**[10], **Raushan T. Kurmasheva, PhD**[11], **David A. Wheeler, PhD**[2,3], and **Peter J. Houghton, PhD**[11]

[1]Cancer Therapy Evaluation Program, NCI, Bethesda, MD

[2]Human Genome Sequencing Center, Baylor College of Medicine, Houston, TX

[3]Department of Molecular and Human Genetics, Baylor College of Medicine, Houston, TX

[4]Texas Tech University Health Sciences Center, Lubbock, TX

[5]Children's Hospital of Philadelphia, University of Pennsylvania School of Medicine and Abramson Family Cancer Research Institute, Philadelphia, PA

[6]The Children's Hospital at Montefiore, Bronx, NY

[7]A.I. duPont Hospital for Children, Wilmington, DE

[8]Children's Cancer Institute Australia for Medical Research, Randwick, NSW, Australia

[9]Duke University Medical Center, Durham, NC

[10]St. Jude Children's Research Hospital, Memphis, TN

[11]Nationwide Children's Hospital, Columbus, OH

Abstract

Introduction—BMN 673 is a potent inhibitor of poly-ADP ribose polymerase (PARP) that is in clinical testing with a primary focus on BRCA-mutated cancers. BMN 673 is active both through inhibiting PARP catalytic activity and by tightly trapping PARP to DNA at sites of single strand breaks.

Methods—BMN 673 was tested in vitro at concentrations ranging from 0.1 nM to 1 μM and in vivo at a daily dose of 0.33 mg/kg administered orally twice daily (Mon-Fri) and once daily on weekends (solid tumors) for 28 days.

Results—The median relative IC_{50} (rIC_{50}) concentration against the PPTP cell lines was 25.8 nM. The median rIC_{50} for the Ewing cell lines was lower than for the remaining cell lines (6.4

Corresponding Author: Malcolm A. Smith, MD, PhD, National Cancer Institute, 9609 Medical Center Drive, RM 5-W414, MSC 9737, Bethesda, MD 20892 (for U.S. Postal Service Delivery), Phone: (240) 276-6087, Malcolm.Smith@nih.gov.

Conflict of Interest Statement: The authors consider that there are no actual or perceived conflicts of interest.

versus 31.1 nM, respectively). In vivo BMN 673 induced statistically significant differences in EFS distribution in 17/43 (39.5%) xenograft models. Three objective regressions were observed: a complete response (CR) in a medulloblastoma line (BT-45), a maintained CR in a Wilms tumor line (KT-10), and a maintained CR in an ependymoma line (BT-41). BMN 673 maintained its high level of activity against KT-10 with a 3-fold reduction in dose. KT-10 possesses a truncating mutation in *PALB2* analogous to *PALB2* mutations associated with hereditary breast and ovarian cancer that abrogate homologous recombination (HR) repair.

Conclusions—The PPTP results suggest that single agent BMN 673 may have limited clinical activity against pediatric cancers. Single agent activity is more likely for patients whose tumors have defects in HR repair.

Keywords

Preclinical Testing; Developmental Therapeutics; PARP inhibitor; PALB2

Introduction

The observation that cancer cells defective in homologous recombination as a consequence of *BRCA1* or *BRCA2* mutations are hypersensitive to inhibitors of poly-ADP ribose polymerase (PARP) has spurred the development of PARP inhibitors. Early clinical trials have demonstrated a high frequency of tumor responses in BRCA-mutant patients [1,2]. In the absence of functional homologous recombination, cells become dependent upon Base Excision Repair (BER) for repair of single strand DNA breaks and repair of apurinic sites within DNA. PARP-1 and -2 play an essential role in BER, and enhanced cytotoxicity associated with PARP inhibition correlates closely with PARP-1 binding to the 5′-deoxyribose phosphate group-containing BER intermediate [3]. PARP binds damaged DNA even in the presence of an inhibitor, and it is considered that the inactive-DNA-bound PARP-1 is persistent, inhibiting the BER process. Inhibition of PARP-1 catalytic activity results in trapping of the enzyme on DNA, as catalytic inhibitors prevent dissociation of PARP from DNA that is required for completion of DNA repair [4]. The cytotoxicity of inhibited PARP-bound to DNA is linked to formation of replication-dependent DNA double strand breaks and induction of both p53-dependent and p53-independent cell death [5].

At least seven PARP inhibitors are in clinical development. BMN 673, (8S,9R)-5-fluoro-8-(4-fluorophenyl)-9-(1-methyl-1H-1,2,4-triazol-5-yl)-8,9-dihydro-2H-pyrido[4,3,2-de]phthalazin-3(7H)-one), is a potent PARP-1/2 inhibitor (PARP-1 IC_{50} = 0.57 nmol/L). Inhibition of PARP-1 and -2 is stereospecific, with one of the trans isomers being a potent inhibitor whereas the other isomer is relatively inactive (IC_{50} > 100nM) [6,7]. The selectivity, and lack of off-target effects for BMN 673 were shown by the lack of cytotoxicity in $PARP^{-/-}$ deficient DT40 cells (that lack PARP-2), whereas wild type DT40 cells were sensitive to nanomolar concentrations of drug [7]. Like other PARP inhibitors such as rucaparib, veliparib, and olaparib, BMN 673 shows inhibition of PARP catalytic activity at nanomolar concentrations [7], but the cytotoxic potency of BMN 673 exceeds that of these other PARP inhibitors by a factor of 10-fold or greater [7]. BMN 673 has completed its phase 1 evaluation with a recommended phase 2 dose of 1 mg/day and with the primary dose-limiting toxicity being thrombocytopenia [8]. Impressive antitumor activity was

observed in BRCA-mutated patients with ovarian cancer and breast cancer [8], and a phase 3 clinical trial is evaluating BMN 673 for patients with germline BRCA mutations and locally advanced and/or metastatic breast cancer (NCT01945775).

Recently, it was demonstrated that Ewing sarcoma cell lines are hypersensitive to PARP inhibition [9], although the mechanism for sensitivity remains unclear. This spurred interest in testing a PARP inhibitor against the in vitro and in vivo panels of the Pediatric Preclinical Testing Program (PPTP). Because of its potency and specificity for PARP-1/2 inhibition, BMN 673 was chosen for testing.

Materials and Methos

In vitro* testing—In vitro* testing was performed using DIMSCAN, a semiautomatic fluorescence-based digital image microscopy system that quantifies viable (using fluorescein diacetate [FDA]) cell numbers in tissue culture multiwell plates [10]. Cells were incubated in the presence of BMN 673 for 96 hours at concentrations from 0.1 nM to 1 μM and analyzed as previously described [11].

The Relative In/Out (I/O)% values compare the relative difference in final cell number compared with the starting cell number for treated cells and for control cells calculated as follows: (Observed $Y_{min}-Y_0$)/(100−Y_0) if Observed $Y_{min}>Y_0$; and (Observed $Y_{min}-Y_0$)/(Y_0) if Observed $Y_{min}<$Predicted Y_{min}). Y_0 is an estimate of the starting cell number derived from determinations of the doubling time for each cell line. Relative I/O% values range between 100% (no treatment effect) to -100% (complete cytotoxic effect), with a Relative I/O% value of 0% being observed for a completely effective cytostatic agent.

In vivo tumor growth inhibition studies—Mouse strains used to propagate solid tumors, glioblastomas and acute lymphoblastic leukemias, and methods for assessing tumor response have been described previously [12-14]. Female mice were used irrespective of the patient gender from which the original tumor was derived. All mice were maintained under barrier conditions and experiments were conducted using protocols and conditions approved by the institutional animal care and use committee of the appropriate consortium member. Eight (leukemias) or 10 (solid tumors) mice were used in each control or treatment group. An in-depth description of the analysis methods is included in the Supplemental Response Definitions section (see Supplemental Materials).

Statistical Methods—The exact log-rank test, as implemented using Proc StatXact for SAS®, was used to compare event-free survival (EFS) distributions between treatment and control groups. P-values were two-sided and were not adjusted for multiple comparisons given the exploratory nature of the studies. The Mann–Whitney test was used to test the difference of medians of rIC_{50} values between the groups of lines with high and low SLFN11 expression levels. The Pearson correlation coefficient for the correlation between SLFN11 expression and rIC_{50} or Relative I/O% was determined using GraphPad Prism 6.03. SLFN11 expression is from Affymetrix U133 Plus 2.0 arrays (probeset 226743_at) as previously described [15].

Drugs and Formulation—BMN 673 was provided to the Pediatric Preclinical Testing Program by the Biomarin Pharmaceutical Inc., through the Cancer Therapy Evaluation Program (NCI). BMN 673 was formulated in dimethylacetamide, Solutol HS15, phosphate buffered saline (10:5:85) and stored up to 7 days at 4°C. The solution was brought to ambient temperature and vortexed prior to oral dosing (P.O.). BMN 673 was administered twice daily (BID) at a daily dose of 0.33 mg/kg for 5 days (Monday-Friday), and once daily at weekends (solid tumors). BMN 673 was provided to each consortium investigator in coded vials for blinded testing.

Results

BMN 673 *in vitro* testing

BMN 673 was tested against the PPTP's *in vitro* cell line panel at concentrations ranging from 0.1 nM to 1 μM. The median relative IC_{50} value for the PPTP cell lines was 25.8 nM, with a range from 3.7 nM (TC-71, Ewing sarcoma) to >1000 nM (BT-12, CHLA-266 rhabdoid tumor lines). The median rIC_{50} for the Ewing cell lines was lower than for the remaining cell lines (6.4 versus 31.1 nM, respectively, p=0.06), and 3 of 4 Ewing cell lines showed 3.5 to 7.7-fold greater sensitivity to BMN 673 compared to the panel median sensitivity (Table I).

BMN 673 demonstrated cytotoxic activity against some cell lines, as evidence by Y_{min} values approaching 0% and Relative I/O% values approaching -100%. This evidence for a cytotoxic effect was most prominent for the ALL and Ewing cell lines (e.g. NALM-6, MOLT-4, CHLA-9, and TC-71). By contrast, the rhabdomyosarcoma cell lines have Relative I/O% (Observed) values near 0%. The Relative I/O% based on Hill equation Y_{min} estimates are similar to the observed Relative I/O% values, consistent with a plateau effect for BMN 673 at higher concentrations.

Schlafen-11 (SLFN11) expression shows a highly significant positive correlation with the response of adult cancer cell lines to multiple classes of cytotoxic agents, including topoisomerase-1 inhibitors, topoisomerase-2 inhibitors, alkylating agents, and DNA synthesis inhibitors [16]. More recently this relationship between cell line sensitivity and SLFN11 expression has been extended to PARP inhibitors [17]. For the PPTP cell lines, SLFN11 expression was not significantly correlated to the BMN 673 potency as measured by rIC_{50} (R^2=0.11, p=0.11). However, SLFN11 expression was significantly correlated to the Relative I/O% value (R^2=0.26, p=0.01) (Figure 1A). Another way of addressing the relationship between Relative I/O% values and SLFN11 expression is to examine the Relative I/O% values for low expressing (< median) and high expressing (> median) cell lines. Cell lines with high expression of SLFN11 show near complete cytotoxicity (median Relative I/O% = -88%) while those with low expression show significantly higher Relative I/O% values consistent with cytostasis (median Relative I/O% = +4%) (p=0.006) (Figure 1B). The Ewing cell lines show significantly higher median SLFN11 expression values compared to the non-Ewing cell lines (p=0.02).

BMN 673 *in vivo* testing

BMN 673 was tested against the PPTP solid tumor xenografts using a daily dose of 0.33 mg/kg administered BID weekdays and SID on weekends by the P.O. route for 28 days. For ALL models the daily dose was 0.33 mg/kg administered BID (Monday-Friday). The total planned treatment and observation period was 6 weeks. BMN 673 was generally well tolerated, with only a 2.2% (8/363) toxicity rate in the solid tumor treated groups compared to 0.3% (1/356) toxicity in control animals. For the ALL xenografts, the toxicity rate for treated animals was 0% (n=71). Forty-four of the 45 tested xenograft models were considered evaluable for efficacy. Complete details of testing are provided in Supplemental Table I.

BMN 673 induced statistically significant differences in EFS distribution compared to control in 17 of 35 (48.6%) of the solid tumor xenografts evaluable for this measure and in 0 of 8 (0%) of the evaluable ALL xenografts Table II. For those xenografts with a significant difference in EFS distribution between treated and control groups, the EFS T/C activity measure additionally requires an EFS T/C value of > 2.0 for intermediate activity and indicates a substantial agent effect in slowing tumor growth. High activity additionally requires a reduction in final tumor volume compared to the starting tumor volume. BMN 673 induced tumor growth inhibition meeting criteria for intermediate/high EFS T/C activity in 2 of 32 (6.3%) solid tumor xenografts evaluable for this measure. These were the Wilms tumor xenograft KT-10 and the rhabdoid tumor xenograft KT-16. For the ALL panel, no xenografts met criteria for intermediate/high activity. The *in vivo* testing results for the objective response measure of activity are presented in Figure 2 in a ‘heat-map’ format as well as a ‘COMPARE’-like format, based on the scoring criteria described in the Supplemental Response Definitions section. The latter analysis demonstrates relative tumor sensitivities around the midpoint score of 5 (stable disease).

KT-10, the medulloblastoma line BT-45, and the ependymoma line BT-41, had MCR, CR, and MCR responses, respectively. BT-41 is a slow-growing xenograft, and the relative tumor volume (RTV) of treated animals decreased to 0.4 at the end of the 6 week treatment/observation period while the control tumor volume only increased to a relative tumor volume (RTV) of 1.7 during the same time period. To further evaluate the response of KT-10 to BMN 673, a dose-response evaluation was performed using daily doses of 0.33, 0.2 and 0.1 mg/kg. All 3 dose levels produced complete responses to 4 weeks of treatment that were maintained for an additional 8 week observation period (Figure 3).

Genomic testing results

Gene mutation profiles of KT-10 and BT-45 were examined to identify genomic factors that might explain the responsiveness of these xenografts to BMN 673 (Supplemental Table II). Gene sequencing methods are provided in the supplemental materials. For BT-45, mutations expected for the WNT subtype of medulloblastoma are observed, including a *CTNNB1* mutation (G34R) and a *TP53* mutation (R248W) [18,19]. For KT-10, the key finding is a frameshift mutation in *Partner And Localizer of BRCA2* (*PALB2*) (c.3323delA leading to p.Y1108fs and to subsequent creation of a p.Stop(*)1122). The nucleotide and amino acid sequence of the normal and mutated *PALB2* are shown in Supplemental Table III. The

mutation occurs in exon 12 of *PALB2* and is homozygous or hemizyous as virtually all *PALB2* reads are for the mutated rather than the wild type allele. Figure 4 shows the Y1108fs mutation identified for KT-10 xenografts as well as other cancer or Fanconi anemia associated *PALB2* mutations reported in the literature, nonsense or frameshift mutations are commonly observed. Of specific relevance to the KT-10 mutation, those that lead to loss of the WD40 domains in the C-terminus of the protein block the ability of *PALB2* to associate with *BRCA2* and are associated with Fanconi anemia and non-*BRCA1/BRCA2* hereditary breast cancer [20-23]. The c.3323delA (Y1108fs) mutation has been reported in a child with Fanconi anemia who developed Wilms tumor [22].

Discussion

Single agent activity for PARP inhibitors has been reported in patients with BRCA-mutant breast cancer [1]. Relative to other cancer cell lines Ewing sarcoma cells were also reported to be sensitive to PARP inhibition, with IC_{50} values comparable to those for BRCA1 mutant cell lines [9]. These observations, along with a proposed mechanism for susceptibility of EWS-FLI1 expressing cancer cells to PARP inhibitors, made us hopeful that we would observe high level activity for single agent BMN 673 against our Ewing sarcoma models.

BMN 673 is a potent stereo-selective inhibitor of PARP-1 and -2, with a IC_{50} against PARP1 IC_{50} of 0.57 nM [6]. In vitro, we demonstrated significant cytotoxic potency with 3 of 4 Ewing sarcoma cell lines being more sensitive than the panel median rIC_{50}, whereas two rhabdoid cell lines were highly refractory. Our results are consistent with the previously reported preferential sensitivity of Ewing cell lines to the PARP inhibitor olaparib [9]. However, the in vitro sensitivity of the Ewing cell lines to BMN 673 did not translate into in vivo activity, as five Ewing xenografts showed minimal growth delay to BMN 673. Most other xenografts tested similarly showed limited response, including the ALL models and most other solid tumor models. Consistent with the in vivo results presented here, a recent phase 2 trial of olaparib failed to show significant activity in Ewing sarcoma patients [24].

We extend results of the Pommier laboratory regarding the relationship between *SLFN11* expression and the in vitro activity of PARP inhibitors like BMN 673 to childhood cancer cell lines [17]. Our results showing a primary effect on Relative I/O% rather than rIC_{50} suggest that the primary effect of *SLFN11* expression is in promoting a cytotoxic rather than a cytostatic response to PARP inhibition. Among the PPTP cell lines, *SLFN11* expression was significantly higher for the Ewing cell lines providing one mechanism that may contribute to the preferential response of Ewing cell lines to PARP inhibitors. Loss of 53BP1 has been shown to confer resistance to the PARP inhibitor olaparib in a BRCA-deficient mouse model of breast cancer, however [25], there was no obvious relationship between in vitro or in vivo sensitivity with expression levels of 53BP1 or p53 genotype. Acquired resistance to olaparib has also been associated with overexpression of ABCB1 [26] that encodes the P-glycoprotein drug efflux pump. It is unlikely that the in vivo resistance to BMN 673 is associated with increased expression of P-glycoprotein, as many of the tumors that fail to respond to BMN 673 are highly responsive to vincristine and eribulin [27,28], antimitotic agents that are established P-glycoprotein substrates.

There were three solid tumors that regressed to treatment with BMN 673, KT-10 (Wilms tumor) and BT-45 (medulloblastoma) and BT-41 (ependymoma). Of note the former two tumors were also sensitive to cisplatin [29], while the latter was not tested against cisplatin. Further testing and molecular analysis of ependymoma xenografts is required to understand the significance of the BT-41 response. The responses to both BMN 673 and to cisplatin are suggestive of a defect in homologous recombination (HR) repair [30]. We did not observe mutations affecting HR repair in BT-45, although we did observe *CTNNB1* and *TP53* mutations suggesting that this xenograft represents the WNT subtype of medulloblastoma [31]. The lack of a mutation in an HR repair gene is not necessarily surprising as illustrated by a recent report for ovarian cancer: while germline or somatic mutation in a HR repair gene was strongly associate with primary platinum sensitivity (71 of 85, 84%), a substantial proportion of patients without identified HR repair gene mutations (95 of 158, 60%) showed platinum sensitivity [30]. Hence, predictive factors for cisplatin sensitivity extend beyond HR repair gene mutations.

The response of BMN 673 to KT-10 is particularly remarkable, as complete responses maintained through 4 weeks of treatment and 8 weeks of follow-up were observed at doses as low as 0.1 mg/kg/day. Consistent with the sensitivity of KT-10 to both BMN 673 and to cisplatin [30,32,33], we identified a frameshift mutation in KT-10 in the gene, *PALB2* [34]. PALB2 binds to both BRCA1 and BRCA2, with the former association occurring through its N-terminal coiled-coil domain and with the latter occurring through its WD40 domains [23,35-38]. Truncation in the C-terminal end of *PALB2* results in loss of its *BRCA2* binding ability, leading to defective HR repair and sensitivity to chromosomal breakage induced by DNA cross-linking agents such as mitomycin C [23]. The presence of biallelic mutations in *PALB2* leads to Fanconi anemia, and an alias for *PALB2* is FANC-N [22,23,39]. Likewise, mutations in *PALB2* that disrupt binding with *BRCA2* are associated with hereditary breast cancer [40], and germline truncating mutations in *PALB2* are observed in pancreatic cancer and ovarian cancer [41,42]. The frameshift mutation that we observed in KT-10 has previously been reported for a patient with Fanconi anemia, confirming the pathogenic nature of the mutation [22].

Our results suggest that *PALB2* mutations will behave similarly to *BRCA1* and *BRCA2* mutations in inducing synthetic lethality with PARP inhibition. This observation is consistent with several prior reports describing in vitro sensitivity of *PALB2* mutations to PARP inhibition. A cell line derived from a patient with Fanconi anemia and a biallelic *PALB2* truncating mutation showed hypersensitivity to the PARP inhibitor olaparib [43,44]. Additionally, a patient with pancreatic cancer and with biallelically inactivated *PALB2* showed a favorable response to mitomycin C, consistent with an HR repair defect [45]. Our report is to our knowledge the first report describing in vivo hypersensitivity of *PALB2*-mutated tumors to PARP inhibition.

The observation of a *PALB2* mutation in Wilms tumor is consistent with the cancer spectrum associated with Fanconi anemia. Wilms tumor and medulloblastoma are the cancers most commonly reported in patients with Fanconi anemia and biallelic *PALB2* mutations [22,23]. Children with Fanconi anemia and biallelic *BRCA2* mutations who develop cancer also show a predominance of Wilms tumor and medulloblastoma [46]. We

do not have data on whether the child from which KT-10 was developed was affected by Fanconi anemia. A cell line derived from a patient with Fanconi anemia and a biallelic *PALB2* truncating mutation showed hypersensitivity to the PARP inhibitor olaparib [43]. Thus, therapy with a PARP inhibitor for cancers arising in patients with Fanconi anemia may not show a therapeutic window as both the host and the cancer will be hypersensitive to PARP inhibition. This caveat would likely not apply to patients heterozygous for *PALB2* mutations who develop cancer as part of a BRCA-like predisposition syndrome.

The data presented suggest that as a single agent BMN 673 may have limited clinical activity against childhood cancers. The observation of limited single agent activity for BMN 673 against Ewing sarcoma xenografts is consistent with clinical experience with olaparib [47]. It is possible that at dose limiting toxicity (the lethality rate was 2.2% at the dose/schedule used for solid tumors, and the dose was reduced due to excessive toxicity for the ALL models), inadequate exposures to BMN 673 were reached in tumor tissue. The in vitro experiments presented demonstrate increased sensitivity of Ewing sarcoma cell lines relative to other cancer cell lines. The data do not compare the sensitivity of Ewing cells to cells from normal tissues. Thus, at least in mice, the failure to elicit responses against Ewing sarcoma models may reflect a lack of therapeutic index for this agent.

BMN 673 single agent activity is more likely for patients whose tumors have defects in HR repair such as the *PALB2* mutation that we describe, with the activity profile likely overlapping that of single agent cisplatin. *PALB2* mutations represent a small proportion of hereditary breast, pancreatic, and ovarian cancer cases [40-42], and our results suggest the potential utility of BMN 673 for these patients. Marked synergy of PARP inhibitors with temozolomide has been reported [3,48,49], as has the ability of certain PARP inhibitors like BMN 673 to trap PARP tightly to DNA following exposure of cells to DNA methylating agents [4,7]. These observations suggest that the combination of BMN 673 with DNA methylating agents may be more efficacious than single agent BMN 673 for selected childhood cancers.

Supplementary Material

Refer to Web version on PubMed Central for supplementary material.

Acknowledgments

This work was supported by NO1-CM-42216, NO1-CM91001-03, CA21765, and CA108786 from the National Cancer Institute and used BMN 673 supplied by BioMarin Pharmaceutical Inc., Novato, CA. In addition to the authors this paper represents work contributed by the following: Sherry Ansher, Joshua Courtright, Edward Favours, Henry S. Friedman, Debbie Payne-Turner, Charles Stopford, Chandra Tucker, Amy E. Watkins, Catherine A. Billups, Joe Zeidner, Ellen Zhang, and Jian Zhang. Children's Cancer Institute Australia for Medical Research is affiliated with the University of New South Wales and Sydney Children's Hospital.

Reference List

1. Tutt A, Robson M, Garber JE, et al. Oral poly(ADP-ribose) polymerase inhibitor olaparib in patients with BRCA1 or BRCA2 mutations and advanced breast cancer: a proof-of-concept trial. Lancet. 2010; 376(9737):235–244. [PubMed: 20609467]

2. Fong PC, Yap TA, Boss DS, et al. Poly(ADP)-ribose polymerase inhibition: frequent durable responses in BRCA carrier ovarian cancer correlating with platinum-free interval. Journal of clinical oncology : official journal of the American Society of Clinical Oncology. 2010; 28(15):2512–2519. [PubMed: 20406929]
3. Horton JK, Wilson SH. Predicting Enhanced Cell Killing through PARP Inhibition. Molecular cancer research : MCR. 2013; 11(1):13–18. [PubMed: 23193155]
4. Murai J, Huang SY, Das BB, et al. Trapping of PARP1 and PARP2 by Clinical PARP Inhibitors. Cancer research. 2012; 72(21):5588–5599. [PubMed: 23118055]
5. Nguyen D, Zajac-Kaye M, Rubinstein L, et al. Poly(ADP-ribose) polymerase inhibition enhances p53-dependent and -independent DNA damage responses induced by DNA damaging agent. Cell Cycle. 2011; 10(23):4074–4082. [PubMed: 22101337]
6. Shen Y, Rehman FL, Feng Y, et al. BMN 673, a novel and highly potent PARP1/2 inhibitor for the treatment of human cancers with DNA repair deficiency. Clinical cancer research : an official journal of the American Association for Cancer Research. 2013; 19(18):5003–5015. [PubMed: 23881923]
7. Murai J, Huang SY, Renaud A, et al. Stereospecific PARP Trapping by BMN 673 and Comparison with Olaparib and Rucaparib. Molecular cancer therapeutics. 2014; 13(2):433–443. [PubMed: 24356813]
8. De Bono JS, Mina LA, Gonzalez M, et al. First-in-human trial of novel oral PARP inhibitor BMN 673 in patients with solid tumors. Journal of clinical oncology : official journal of the American Society of Clinical Oncology. 2013; 31 suppl; abstr 2580.
9. Garnett MJ, Edelman EJ, Heidorn SJ, et al. Systematic identification of genomic markers of drug sensitivity in cancer cells. Nature. 2012; 483(7391):570–575. [PubMed: 22460902]
10. Frgala T, Kalous O, Proffitt RT, et al. A fluorescence microplate cytotoxicity assay with a 4-log dynamic range that identifies synergistic drug combinations. Molecular cancer therapeutics. 2007; 6(3):886–897. [PubMed: 17363483]
11. Houghton PJ, Morton CL, Kolb EA, et al. Initial testing (stage 1) of the proteasome inhibitor bortezomib by the pediatric preclinical testing program. Pediatric Blood & Cancer. 2007; 9999(9999) n/a.
12. Houghton PJ, Morton CL, Tucker C, et al. The pediatric preclinical testing program: Description of models and early testing results. Pediatr Blood Cancer. 2006
13. Friedman HS, Colvin OM, Skapek SX, et al. Experimental chemotherapy of human medulloblastoma cell lines and transplantable xenografts with bifunctional alkylating agents. Cancer research. 1988; 48(15):4189–4195. [PubMed: 3390813]
14. Liem NL, Papa RA, Milross CG, et al. Characterization of childhood acute lymphoblastic leukemia xenograft models for the preclinical evaluation of new therapies. Blood. 2004; 103(10):3905–3914. [PubMed: 14764536]
15. Neale G, Su X, Morton CL, et al. Molecular characterization of the Pediatric Preclinical Testing panel. Clinical cancer research : an official journal of the American Association for Cancer Research. 2008; 14(14):4572–4583. [PubMed: 18628472]
16. Zoppoli G, Regairaz M, Leo E, et al. Putative DNA/RNA helicase Schlafen-11 (SLFN11) sensitizes cancer cells to DNA-damaging agents. Proceedings of the National Academy of Sciences of the United States of America. 2012; 109(37):15030–15035. [PubMed: 22927417]
17. Murai, J.; Josse, R.; Doroshow, JH., et al. Schlafen 11 (SLFN11) is a critical determinant of cellular sensitivity to PARP inhibitors. Proceedings of the 105th Annual Meeting of the American Association for Cancer Research; 2014 Apr 5-9; San Diego, CA Philadelphia (PA). AACR 2014: Abstr #1718
18. Taylor MD, Northcott PA, Korshunov A, et al. Molecular subgroups of medulloblastoma: the current consensus. Acta neuropathologica. 2012; 123(4):465–472. [PubMed: 22134537]
19. Zhukova N, Ramaswamy V, Remke M, et al. Subgroup-specific prognostic implications of TP53 mutation in medulloblastoma. Journal of clinical oncology : official journal of the American Society of Clinical Oncology. 2013; 31(23):2927–2935. [PubMed: 23835706]
20. Erkko H, Xia B, Nikkila J, et al. A recurrent mutation in PALB2 in Finnish cancer families. Nature. 2007; 446(7133):316–319. [PubMed: 17287723]

21. Rahman N, Seal S, Thompson D, et al. PALB2, which encodes a BRCA2-interacting protein, is a breast cancer susceptibility gene. Nature genetics. 2007; 39(2):165–167. [PubMed: 17200668]
22. Reid S, Schindler D, Hanenberg H, et al. Biallelic mutations in PALB2 cause Fanconi anemia subtype FA-N and predispose to childhood cancer. Nature genetics. 2007; 39(2):162–164. [PubMed: 17200671]
23. Xia B, Dorsman JC, Ameziane N, et al. Fanconi anemia is associated with a defect in the BRCA2 partner PALB2. Nature genetics. 2007; 39(2):159–161. [PubMed: 17200672]
24. Choy, E.; Butrynski, JE.; Harmon, D., et al. Translation of preclinical predictive sensitivity of Ewing sarcoma to PARP inhibition: Phase II study of olaparib in adult patients with recurrent/metastatic Ewing sarcoma following failure of prior chemotherapy. Proceedings of the 104th Annual Meeting of the American Association for Cancer Research; 2013; Abstr #LB-174
25. Jaspers JE, Kersbergen A, Boon U, et al. Loss of 53BP1 causes PARP inhibitor resistance in Brca1-mutated mouse mammary tumors. Cancer discovery. 2013; 3(1):68–81. [PubMed: 23103855]
26. Rottenberg S, Jaspers JE, Kersbergen A, et al. High sensitivity of BRCA1-deficient mammary tumors to the PARP inhibitor AZD2281 alone and in combination with platinum drugs. Proceedings of the National Academy of Sciences of the United States of America. 2008; 105(44): 17079–17084. [PubMed: 18971340]
27. Houghton PJ, Morton CL, Tucker C, et al. The pediatric preclinical testing program: description of models and early testing results. Pediatr Blood Cancer. 2007; 49(7):928–940. [PubMed: 17066459]
28. Kolb EA, Gorlick R, Reynolds CP, et al. Initial testing (stage 1) of eribulin, a novel tubulin binding agent, by the pediatric preclinical testing program. Pediatr Blood Cancer. 2013; 60(8):1325–1332. [PubMed: 23553917]
29. Tajbakhsh M, Houghton PJ, Morton CL, et al. Initial testing of cisplatin by the Pediatric Preclinical Testing Program. Pediatr Blood Cancer. 2008; 50(5):992–1000. [PubMed: 17554786]
30. Pennington KP, Walsh T, Harrell MI, et al. Germline and somatic mutations in homologous recombination genes predict platinum response and survival in ovarian, fallopian tube, and peritoneal carcinomas. Clinical cancer research : an official journal of the American Association for Cancer Research. 2014; 20(3):764–775. [PubMed: 24240112]
31. Kool M, Korshunov A, Remke M, et al. Molecular subgroups of medulloblastoma: an international meta-analysis of transcriptome, genetic aberrations, and clinical data of WNT, SHH, Group 3, and Group 4 medulloblastomas. Acta neuropathologica. 2012; 123(4):473–484. [PubMed: 22358457]
32. Bryant HE, Schultz N, Thomas HD, et al. Specific killing of BRCA2-deficient tumours with inhibitors of poly(ADP-ribose) polymerase. Nature. 2005; 434(7035):913–917. [PubMed: 15829966]
33. Farmer H, McCabe N, Lord CJ, et al. Targeting the DNA repair defect in BRCA mutant cells as a therapeutic strategy. Nature. 2005; 434(7035):917–921. [PubMed: 15829967]
34. Tischkowitz M, Xia B. PALB2/FANCN: recombining cancer and Fanconi anemia. Cancer research. 2010; 70(19):7353–7359. [PubMed: 20858716]
35. Tischkowitz M, Xia B, Sabbaghian N, et al. Analysis of PALB2/FANCN-associated breast cancer families. Proceedings of the National Academy of Sciences of the United States of America. 2007; 104(16):6788–6793. [PubMed: 17420451]
36. Sy SM, Huen MS, Chen J. PALB2 is an integral component of the BRCA complex required for homologous recombination repair. Proceedings of the National Academy of Sciences of the United States of America. 2009; 106(17):7155–7160. [PubMed: 19369211]
37. Zhang F, Fan Q, Ren K, et al. PALB2 functionally connects the breast cancer susceptibility proteins BRCA1 and BRCA2. Molecular cancer research : MCR. 2009; 7(7):1110–1118. [PubMed: 19584259]
38. Oliver AW, Swift S, Lord CJ, et al. Structural basis for recruitment of BRCA2 by PALB2. EMBO reports. 2009; 10(9):990–996. [PubMed: 19609323]
39. Patel KJ. Fanconi anemia and breast cancer susceptibility. Nature genetics. 2007; 39(2):142–143. [PubMed: 17262024]

40. Fernandes PH, Saam J, Peterson J, et al. Comprehensive sequencing of PALB2 in patients with breast cancer suggests PALB2 mutations explain a subset of hereditary breast cancer. Cancer. 2014; 120(7):963–967. [PubMed: 24415441]

41. Kanchi KL, Johnson KJ, Lu C, et al. Integrated analysis of germline and somatic variants in ovarian cancer. Nature communications. 2014; 5:3156.

42. Jones S, Hruban RH, Kamiyama M, et al. Exomic sequencing identifies PALB2 as a pancreatic cancer susceptibility gene. Science. 2009; 324(5924):217. [PubMed: 19264984]

43. Park JY, Singh TR, Nassar N, et al. Breast cancer-associated missense mutants of the PALB2 WD40 domain, which directly binds RAD51C, RAD51 and BRCA2, disrupt DNA repair. Oncogene. 2013

44. Buisson R, Dion-Cote AM, Coulombe Y, et al. Cooperation of breast cancer proteins PALB2 and piccolo BRCA2 in stimulating homologous recombination. Nature structural & molecular biology. 2010; 17(10):1247–1254.

45. Villarroel MC, Rajeshkumar NV, Garrido-Laguna I, et al. Personalizing cancer treatment in the age of global genomic analyses: PALB2 gene mutations and the response to DNA damaging agents in pancreatic cancer. Molecular cancer therapeutics. 2011; 10(1):3–8. [PubMed: 21135251]

46. Alter BP, Rosenberg PS, Brody LC. Clinical and molecular features associated with biallelic mutations in FANCD1/BRCA2. Journal of medical genetics. 2007; 44(1):1–9. [PubMed: 16825431]

47. Choy, E.; Butrynski, JE.; Harmon, D., et al. Translation of preclinical predictive sensitivity of Ewing sarcoma to PARP inhibition: Phase II study of olaparib in adult patients with recurrent/metastatic Ewing sarcoma following failure of prior chemotherapy. Proceedings of the 104th Annual Meeting of the American Association for Cancer Research; 2013; Abstr #LB-174

48. Brenner JC, Feng FY, Han S, et al. PARP-1 inhibition as a targeted strategy to treat Ewing's sarcoma. Cancer research. 2012; 72(7):1608–1613. [PubMed: 22287547]

49. Norris RE, Adamson PC, Nguyen VT, et al. Preclinical evaluation of the PARP inhibitor, olaparib, in combination with cytotoxic chemotherapy in pediatric solid tumors. Pediatr Blood Cancer. 2014; 61(1):145–150. [PubMed: 24038812]

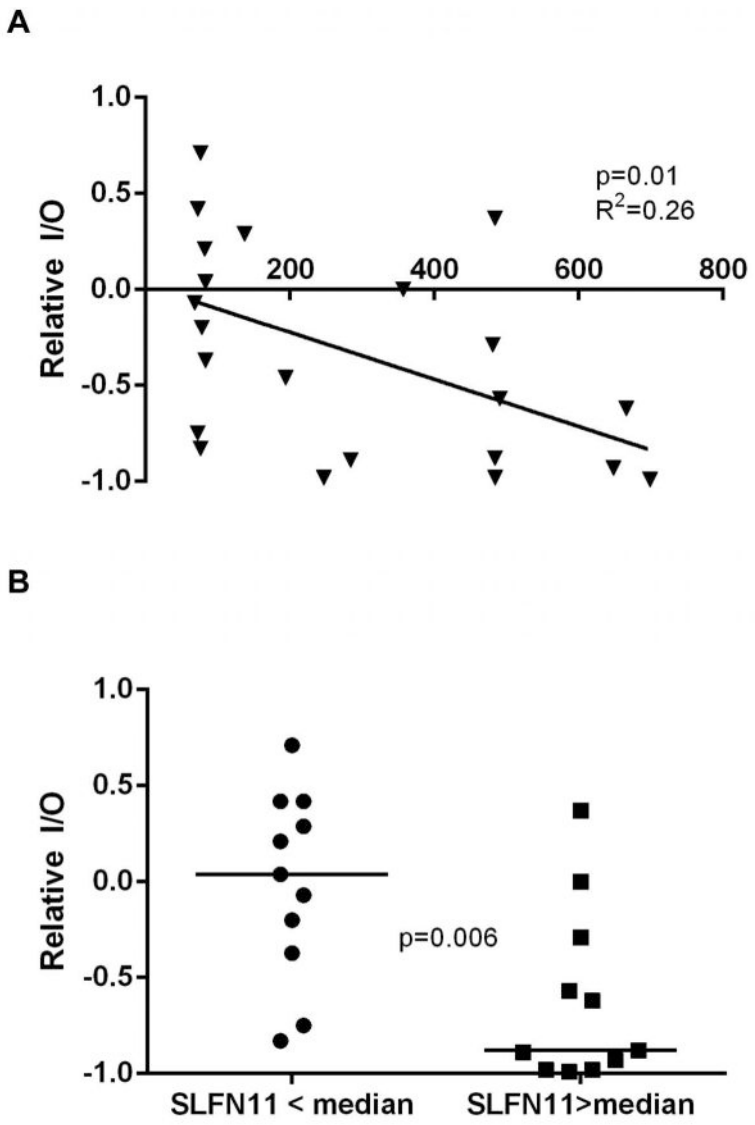

Figure 1.

(A) Correlation between SLFN11 expression values (x-axis) and Relative I/O values expressed numerically rather than as percents (ranging from -1.0 as complete cytotoxicity to +1.0 as no treatment effect, with 0 as cytostasis). (B) Median Relative I/O values for PPTP cell lines for lines with low SLFN11 expression (<median) and with high SLFN11 expression (>median).

Xenograft Line	Histology	Log-rank p-value	Median Score	Midpoint Difference	Overall Group Response	Heat Map
BT-29	Rhabdoid	0.299	0	-5	PD1	
KT-16	Rhabdoid	**0.007**	2	-3	PD2	
KT-14	Rhabdoid	**0.001**	0	-5	PD1	
KT-10	Wilms	**<0.001**	10	5	MCR	
KT-11	Wilms	0.225	1	-4	PD1	
KT-13	Wilms	**0.002**	1	-4	PD1	
SK-NEP-1	Ewing	0.320	0	-5	PD1	
EW5	Ewing	0.454	0	-5	PD1	
EW8	Ewing	**0.009**	0	-5	PD1	
TC-71	Ewing	**<0.001**	1	-4	PD1	
CHLA258	Ewing	**<0.001**	0	-5	PD1	
CHLA258-R	Ewing	**0.002**	2	-3	PD2	
Rh10	Alveolar RMS	0.135	0	-5	PD1	
Rh28	Alveolar RMS	0.362	0	-5	PD1	
Rh30	Alveolar RMS	**0.007**	2	-3	PD2	
Rh30R	Alveolar RMS	0.452	0	-5	PD1	
Rh41	Alveolar RMS	0.440	0	-5	PD1	
Rh18	Embryonal RMS	**0.021**	0	-5	PD1	
BT-28	Medulloblastoma	**0.047**	0	-5	PD1	
BT-45	Medulloblastoma	**<0.001**	8	3	CR	
BT-50	Medulloblastoma	**0.033**	0	-5	PD1	
BT-36	Ependymoma	0.102	2	-3	PD2	
BT-41	Ependymoma	1.000	10	5	MCR	
BT-39	Glioblastoma	0.168	0	-5	PD1	
D645	Glioblastoma	**0.007**	1	-4	PD1	
D456	Glioblastoma	**<0.001**	2	-3	PD2	
NB-SD	Neuroblastoma	0.160	0	-5	PD1	
NB-1691	Neuroblastoma	0.056	0	-5	PD1	
NB-EBc1	Neuroblastoma	0.144	0	-5	PD1	
CHLA-79	Neuroblastoma	0.993	0	-5	PD1	
NB-1643	Neuroblastoma	0.131	0	-5	PD1	
OS-1	Osteosarcoma	**0.005**	0	-5	PD1	
OS-2	Osteosarcoma	**<0.001**	0	-5	PD1	
OS-17	Osteosarcoma	0.551	0	-5	PD1	
OS-33	Osteosarcoma	**<0.001**	0	-5	PD1	
OS-31	Osteosarcoma	0.158	0	-5	PD1	
ALL-2	ALL B-precursor	**0.003**	0	-5	PD1	
ALL-4	ALL B-precursor	**0.021**	0	-5	PD1	
ALL-7	ALL B-precursor	0.153	0	-5	PD1	
ALL-8	ALL T-cell	**0.005**	0	-5	PD1	
ALL-17	ALL B-precursor	0.302	0	-5	PD1	
ALL-19	ALL B-precursor	0.619	0	-5	PD1	
ALL-31	ALL T-cell	0.107	0	-5	PD1	
MLL-7	ALL MLL Infant	0.186	0	-5	PD1	
	Median		**0.0**			
	PD1		**PR**			
	PD2		**CR**			
	SD		**MCR**			

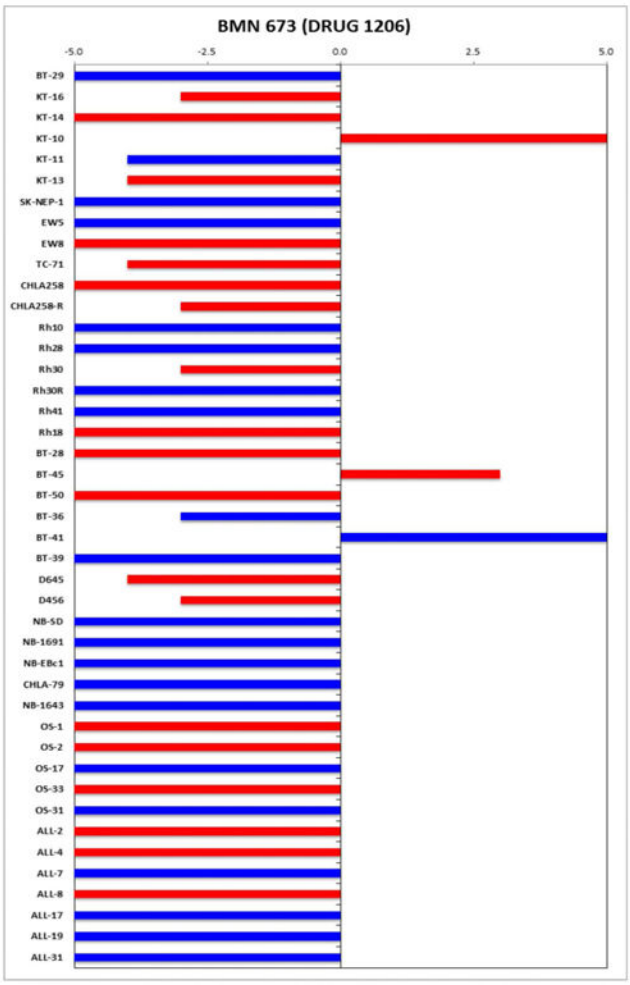

Figure 2.

Left: The colored heat map depicts group response scores. A high level of activity is indicated by a score of 6 or more, intermediate activity by a score of ≥2 but <6, and low activity by a score of <2. Right: representation of tumor sensitivity based on the difference of individual tumor lines from the midpoint response (stable disease). Bars to the right of the median represent lines that are more sensitive, and to the left are tumor models that are less sensitive. Red bars indicate lines with a significant difference in EFS distribution between treatment and control groups, while blue bars indicate lines for which the EFS distributions were not significantly different.

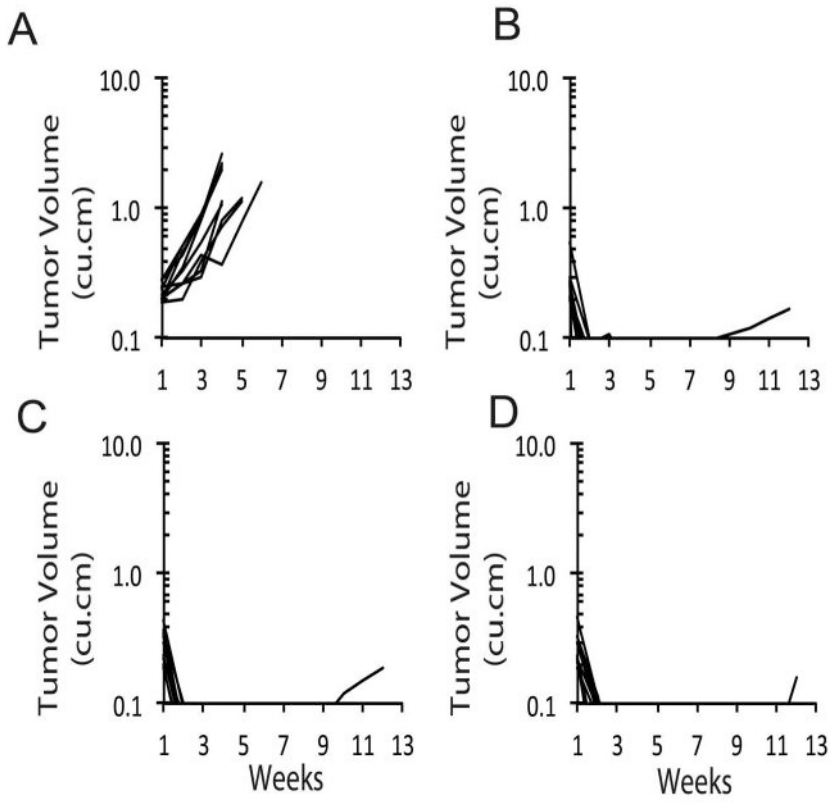

Figure 3.

Sensitivity of KT-10 xenografts to BMN 673. A, Control; B, 0.1625 mg/kg BID (M-F) and 0.33 mg/g SID at weekends; C, 0.1 mg/kg BID and 0.2 SID; D, 0.05 mg/kg BID and 0.1 mg/kg SID on weekends. Mice were treated for 28 days.

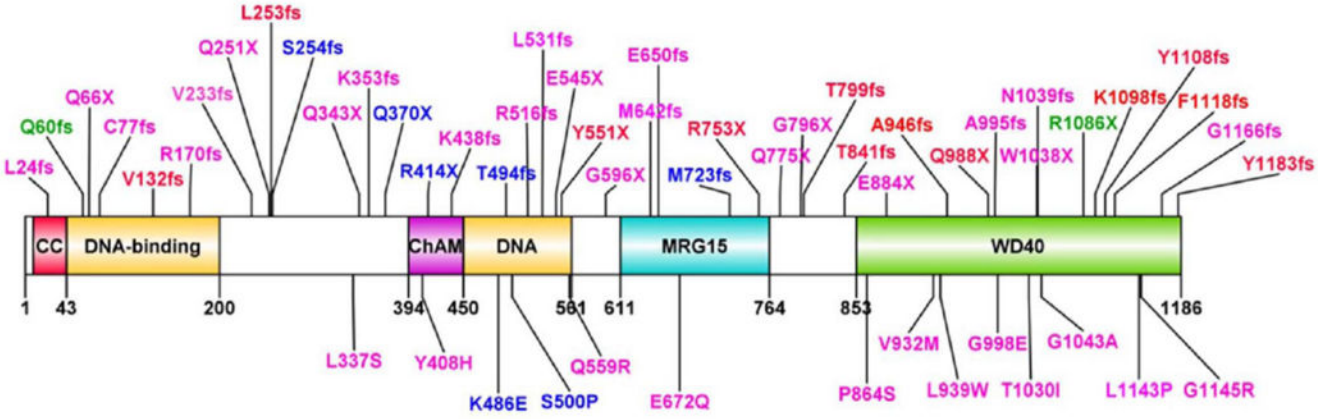

Figure 4.

Disease-associated mutations in PALB2, including the c.3323delA (p.Y1108fs) mutation observed for KT-10. Frame shift and nonsense mutations are depicted above the PALB2 protein schematic, while missense mutations are shown below. Breast-cancer associated mutations are shown in purple font, Fanconi anemia mutations in red font, pancreatic cancer mutations in green font, and ovarian cancer mutations in blue font. A listing of mutations and references is provided in Supplemental Table IV.

Table I

In vitro activity of BMN 673 against PPTP cell lines.

Cell Line	Histotype	rIC_{50} (nM)	Panel rIC_{50}/Line rIC_{50}	Ymin (Observed)	Relative I/O% (Observed Ymin)	SLFN11 Expression
RD	Rhabdomyosarcoma	8.7	3.26	32.6	29%	137
Rh41	Rhabdomyosarcoma	8.1	3.50	20.6	-7%	68
Rh18	Rhabdomyosarcoma	4.9	5.75	28.0	-37%	83
Rh30	Rhabdomyosarcoma	31.1	0.91	16.8	0%	357
BT-12	Rhabdoid	>1,000	0.03	72.9	71%	76
CHLA-266	Rhabdoid	>1,000	0.03	57.3	42%	72
TC-71	Ewing sarcoma	3.7	7.71	0.2	-88%	484
CHLA-9	Ewing sarcoma	8.2	3.48	0.3	-93%	648
CHLA-10	Ewing sarcoma	67.8	0.42	4.4	-29%	481
CHLA-258	Ewing sarcoma	4.6	6.16	15.0	-62%	666
SJ-GBM2	Glioblastoma	16.2	1.75	5.3	-46%	194
NB-1643	Neuroblastoma	18.4	1.55	3.6	-83%	76
NB-EBc1	Neuroblastoma	25.8	1.10	2.4	-89%	284
CHLA-90	Neuroblastoma	>1,000	0.03	57.9	42%	73
CHLA-136	Neuroblastoma	14.2	2.01	7.2	-75%	72
NALM-6	ALL	49.0	0.58	0.0	-99%	699
COG-LL-317	ALL	9.4	3.04	0.1	-98%	247
RS4;11	ALL	52.6	0.54	6.5	-57%	491
MOLT-4	ALL	16.6	1.72	0.2	-98%	484
CCRF-CEM	ALL	697.3	0.04	40.7	37%	484
Kasumi-1	AML	786.2	0.04	43.9	21%	82
Karpas-299	ALCL	75.7	0.38	6.2	-20%	78
Ramos-RA1	NHL	68.3	0.42	5.2	4%	83
Median		**25.8**	**1.10**	**6.5**	**-37%**	**194**
Minimum		**3.7**	**0.03**	**0.0**	**-99%**	**68**
Maximum		**>1,000**	**7.71**	**72.9**	**71%**	**699**

rIC_{50}: relative inhibitory concentration 50; Y_{min}: minimal survival fraction at the highest concentration tested; Relative I/O%: Relative In/Out% (see Methods Section for definition).

Table II

Activity of BMN 673 against the PPTP *in vivo* panel.

Line	Tumor Type	Median Time to Event	P-value	EFS T/C	Median Final RTV/CD45	Tumor Volume T/C	EFS Activity	Objective Response
BT-29	Rhabdoid	31.7	0.299	1.0	>4	0.90	Low	PD1
KT-16	Rhabdoid	21.6	**0.007**	**2.5**	>4	0.61	Int	PD2
KT-14	Rhabdoid	35.5	**0.001**	1.4	>4	0.79	Low	PD1
KT-10	Wilms	> EP	<**0.001**	> **3.8**	0.0	0.00	High	MCR
KT-11	Wilms	23.4	0.225	1.5	>4	0.61	Low	PD1
KT-13	Wilms	18.5	**0.002**	1.5	>4	0.54	Low	PD1
SK-NEP-1	Ewing	14.6	0.320	1.1	>4	0.93	Low	PD1
EW5	Ewing	7.7	0.454	1.1	>4	0.90	Low	PD1
EW8	Ewing	12.2	0.009	.	>4	1.53	**NE**	PD1
TC-71	Ewing	15.2	<**0.001**	1.6	>4	0.50	Low	PD1
CHLA258	Ewing	13.3	<**0.001**	1.4	>4	0.53	Low	PD1
CHLA258	Ewing	17.1	**0.002**	1.8	>4	0.37	Low	PD2
Rh10	Alveolar RMS	17.8	0.135	1.1	>4	0.84	Low	PD1
Rh28	Alveolar RMS	27.6	0.362	0.8	>4	1.24	Low	PD1
Rh30	Alveolar RMS	13.0	**0.007**	1.9	>4	0.63	Low	PD2
Rh30R	Alveolar RMS	16.2	0.452	1.0	>4	1.03	Low	PD1
Rh41	Alveolar RMS	9.7	0.440	1.4	>4	0.88	Low	PD1
Rh18	Embryonal RMS	13.5	**0.021**	1.1	>4	0.89	Low	PD1
BT-28	Medulloblastoma	11.3	**0.047**	1.2	>4	0.83	Low	PD1
BT-45	Medulloblastoma	> EP	<**0.001**	> 1.3	0.7	0.22	**NE**	CR
BT-50	Medulloblastoma	36.6	**0.033**	1.1	>4	0.95	Low	PD1
BT-36	Ependymoma	> EP	0.102	> 1.1	2.7	0.64	**NE**	PD2
BT-41	Ependymoma	>EP	1	.	0.4	0.33	**NE**	MCR
BT-39	Glioblastoma	9.8	0.168	0.9	>4	1.16	Low	PD1
D645	Glioblastoma	8.7	**0.007**	1.4	>4	0.72	Low	PD1
D456	Glioblastoma	7.2	<**0.001**	1.6	>4	0.52	Low	PD2
NB-SD	Neuroblastoma	12.4	0.160	0.9	>4	1.18	Low	PD1
NB-1691	Neuroblastoma	6.0	0.056	1.1	>4	0.83	Low	PD1

Line	Tumor Type	Median Time to Event	P-value	EFS T/C	Median Final RTV/CD45	Tumor Volume T/C	EFS Activity	Objective Response
NB-EBc1	Neuroblastoma	5.2	0.144	1.2	>4	0.68	Low	PD1
CHLA-79	Neuroblastoma	7.7	0.993	1.1	>4	0.97	Low	PD1
NB-1643	Neuroblastoma	7.7	0.131	1.3	>4	0.71	Low	PD1
OS-1	Osteosarcoma	16.5	**0.005**	1.1	>4	0.87	Low	PD1
OS-2	Osteosarcoma	21.1	<**0.001**	1.3	>4	0.76	Low	PD1
OS-17	Osteosarcoma	17.9	0.551	1.1	>4	0.98	Low	PD1
OS-33	Osteosarcoma	18.3	<**0.001**	1.2	>4	0.86	Low	PD1
OS-31	Osteosarcoma	18.3	0.158	1.1	>4	0.88	Low	PD1
ALL-2	ALL B-precursor	9.9	**0.003**	0.6	>25	.	Low	PD1
ALL-4	ALL B-precursor	3.5	**0.021**	0.7	>25	.	Low	PD1
ALL-7	ALL B-precursor	4.3	0.153	0.7	>25	.	Low	PD1
ALL-8	ALL T-cell	5.5	**0.005**	0.5	>25	.	Low	PD1
ALL-17	ALL B-precursor	5.3	0.302	0.6	>25	.	Low	PD1
ALL-19	ALL B-precursor	3.5	0.619	1.1	>25	.	Low	PD1
ALL-31	ALL T-cell	5.3	0.107	0.5	>25	.	Low	PD1
MLL-7	ALL MLL	3.9	0.186	0.9	>25	.	Low	PD1

Event: 4-fold increase in tumor volume. **EFS T/C**: Ratio of median time to event for treated versus control animals. **RTV**: Relative tumor volume (ratio to day 1 tumor volume). **T/C**: Ratio of average tumor volume of treated versus control tumors on last measurement date before any animal in treated or control groups reached “event” status. **PD1** (Progressive Disease 1): >25% ↑ in tumor volume, EFS T/C value ≤1.5. **PD2** (Progressive Disease 2): >25% increase in tumor volume, EFS T/C value >1.5.